Water Research 229 (2023) 119385

Contents lists available at ScienceDirect

Water Research

journal homepage: www.elsevier.com/locate/watres

Generation of reproducible model freshwater particulate matter analogues to study the interaction with particulate contaminants

Helene Walch [a,1], Antonia Praetorius [a,b], Frank von der Kammer [a,*], Thilo Hofmann [a,*]

[a] Department of Environmental Geosciences, Centre for Microbiology and Environmental Systems Science, University of Vienna, Josef-Holaubek-Platz 2, UZA II, 1090 Vienna, Austria

[b] Department of Ecosystem & Landscape Dynamics, Institute for Biodiversity and Ecosystem Dynamics, University of Amsterdam, Science Park 904, 1098 XH Amsterdam, the Netherlands

ARTICLE INFO

Keywords:
Suspended particulate matter
Analogues
Flocs
Particulate contaminants
Fate
Heteroagglomeration

ABSTRACT

Aquatic fate models and risk assessment require experimental information on the potential of contaminants to interact with riverine suspended particulate matter (SPM). While for dissolved contaminants partition or sorption coefficients are used, the underlying assumption of chemical equilibrium is invalid for particulate contaminants, such as engineered nanomaterials, incidental nanoparticles, micro- or nanoplastics. Their interactions with SPM are governed by physicochemical forces between contaminant-particle and SPM surfaces. The availability of a standard SPM material is thus highly relevant for the development of reproducible test systems to evaluate the fate of particulate contaminants in aquatic systems. Finding suitable SPM analogues, however, is challenging considering the complex composition of natural SPM, which features floc-like structures comprising minerals and organic components from the molecular to the microorganism level. Complex composition comes with a heterogeneity in physicochemical surface properties, that cannot be neglected. We developed a procedure to generate SPM analogue flocs from components selected to represent the most abundant and crucial constituents of natural riverine SPM, and the process-relevant SPM surface characteristics regarding interactions with particulate contaminants. Four components, i.e., illite, hematite, quartz and tryptophan, combined at environmentally realistic mass-ratios, were associated to complex flocs. Flocculation was reproducible regarding floc size and fractal dimension, and multiple tests on floc resilience towards physical impacts (agitation, sedimentation-storage-resuspension, dilution) and hydrochemical changes (pH, electrolytes, dissolved organic matter concentration) confirmed their robustness. These reproducible, ready-to-use SPM analogue flocs will strongly support future research on emerging particulate contaminants.

1. Introduction

River-systems are among the major contaminant-receiving waters and constitute potential long-range environmental transport routes. Contaminant transport and fate depend on their interactions with natural materials, which are present in all forms – from truly dissolved, through colloidal and suspended particulate matter, to bed load and bottom sediments. Within this continuum of matter, a crucial role can be attributed to suspended particulate matter (SPM) because (1) SPM is in constant exchange with all other phases, through adsorption/desorption, attachment/detachment, (de-)agglomeration, flocculation/rupture and sedimentation/resuspension, (2) SPM is mobile and links the pelagic and benthic zones (by sedimentation and resuspension), rivers to lakes and oceans (by advective transport) and terrestrial to aquatic environments (via erosion and runoff, or flooding), and (3) SPM provides habitat and feed to aquatic organisms (Walch et al., 2022). The affinity

Abbreviations: SPM, suspended particulate matter; NOM, natural organic matter; EPS, extracellular polymeric substances; FeOx, iron oxides and (oxy)hydroxide minerals; SR-NOM, Suwannee River natural organic matter; TOC, total organic carbon; SEM, scanning electron microscopy; $d_{V0.5}$, volume-based median diameter; D_f, mass fractal dimension; mode d_V, volume-based mode diameter; SPMzero, SPM analogues generated without electrolyte or SR-NOM addition; RSD, relative standard deviation; ave, average; sd, standard deviation.

* Corresponding authors.

E-mail addresses: h.walch@gmx.at, helene.walch@umweltbundesamt.at (H. Walch), a.praetorius@uva.nl (A. Praetorius), frank.kammer@univie.ac.at (F. von der Kammer), thilo.hofmann@univie.ac.at (T. Hofmann).

[1] Present Address: Studies & Consulting, Laboratories, Environment Agency Austria, Spittelauer Lände 5, 1090 Vienna, Austria

https://doi.org/10.1016/j.watres.2022.119385
Received 29 August 2022; Received in revised form 13 November 2022; Accepted 17 November 2022
Available online 19 November 2022

of contaminants for SPM depends on both their respective properties, and governs their transport behavior, bioavailability, uptake, and fate (Geitner et al., 2016; Hofmann and von der Kammer, 2009; Schulze et al., 2015).

A quantification of contaminant-SPM interactions is needed for exposure assessment in the framework of environmental risk assessment. For dissolved contaminants, classical solid/liquid partition coefficients (K_d) can be employed to describe the affinity of a contaminant for water versus solid phases. Over the past decades, however, particulate contaminants, such as engineered nanomaterials, micro- or nanoplastics, received increased attention, and chemical legislation (e.g., REACH, TSCA) requiring environmental risk assessment is adapted to cover these contaminants. This has triggered scientific debate about suitable fate descriptors for particulate contaminants (Dale et al., 2015; Praetorius et al., 2014b; Svendsen et al., 2020; Westerhoff and Nowack, 2013). Praetorius et al. (2014) emphasized that partition coefficients cannot be employed for particulate contaminants, as the underlying thermodynamic equilibrium assumption is only applicable for dissolved substances. Consequently, calls for harmonized testing protocols specific to particulate contaminants (Baun et al., 2017; Stone et al., 2010) can only be responded to while accounting for the process-relevant interaction mechanisms.

Interactions between particulate contaminants and SPM (i.e., heteroagglomeration) are kinetically driven (Praetorius et al., 2014b) and governed by short-range physicochemical surface interactions. As depicted in Fig. 1, interaction forces (mainly electrostatic, hydrophobic, and van der Waals forces, or NOM-interactions) arise from the interplay of intrinsic material properties of both, particulate contaminants and SPM, and hydrochemical conditions (mainly pH, electrolytes, and NOM: natural organic matter) (Elimelech et al., 1995; Gregory, 2005). The effects of intrinsic and extrinsic factors cannot be easily disentangled, especially regarding more complex multi-component systems (Praetorius et al., 2020). Consequently, protocols to test particulate contaminants' affinity for SPM require accounting for both, the process-relevant physicochemical surface properties of natural SPM and the relevant hydrochemical conditions.

Freshwater hydrochemical conditions were recently operationalized within the OECD test guideline No. 318 *Dispersion stability of nanomaterials in simulated environmental media* (OECD, 2017) and the rationale beyond the selected hydrochemical test parameter ranges (Abdolahpur Monikh et al., 2018) is directly applicable to heteroagglomeration. Hence, the selection of suitable counterparts for heteroagglomeration, ideally SPM analogues which represent the agglomeration-relevant natural properties, remains one major gap to fill (Praetorius et al., 2020). Achieving this task is hampered by the complexity and spatiotemporal variability of natural riverine SPM (Walch et al., 2022). SPM is operationally defined and comprises any materials that do not sediment under the given hydrodynamic and hydrochemical conditions and get retained by 0.45 or 0.22 μm filtration membranes (Eisma, 1993). SPM typically exhibits agglomerate or floc-like structures, integrating minerals and organic components (from molecules, via detritus up to microorganisms) of alloch- and autochthonous origins (Droppo, 2001; Henning et al., 2001; Zimmermann--Timm, 2002), with each component contributing distinct physicochemical surface properties to a floc (Walch et al., 2022).

Most heteroagglomeration studies either employed simple mineral SPM surrogates (e.g., Gallego-Urrea et al., 2016; Labille et al., 2015; Oriekhova and Stoll, 2018; Praetorius et al., 2014a; Yu et al., 2021; Zhou et al., 2012) or natural water samples (e.g., Quik et al., 2014; Velzeboer et al., 2014; Adam et al., 2016; Li et al., 2019; Surette and Nason, 2019), but neither meet the need for environmentally relevant and yet standardizable test conditions. Simple minerals do not reflect the complexity and heterogeneity of natural SPM, while natural samples do not allow for reproducibility, since the properties of natural SPM are specific to a certain sampling location and time. So far, the only publication reporting near-natural SPM is Slomberg et al. (2016), who tried to assemble SPM analogues based on the mineralogical composition of SPM from the Rhône catchment. However, they included only major (negatively charged) mineral fractions, neglecting minor but functionally important components such as positively charged oxide and (oxy) hydroxide minerals, or microbial extracellular polymeric substances (EPS) (Walch et al., 2022).

Standardization requires simplification, but a valid model test system needs to cover the most relevant factors which control the process under observation. Hence, we took a conceptual approach to select key components for the generation of complex SPM analogue flocs, developed a simple protocol for their association, and finally evaluated their robustness and handling in the laboratory. The detailed rationale beyond component selection is given in the conceptual framework (supporting information S1). Briefly, we aimed at tailoring SPM

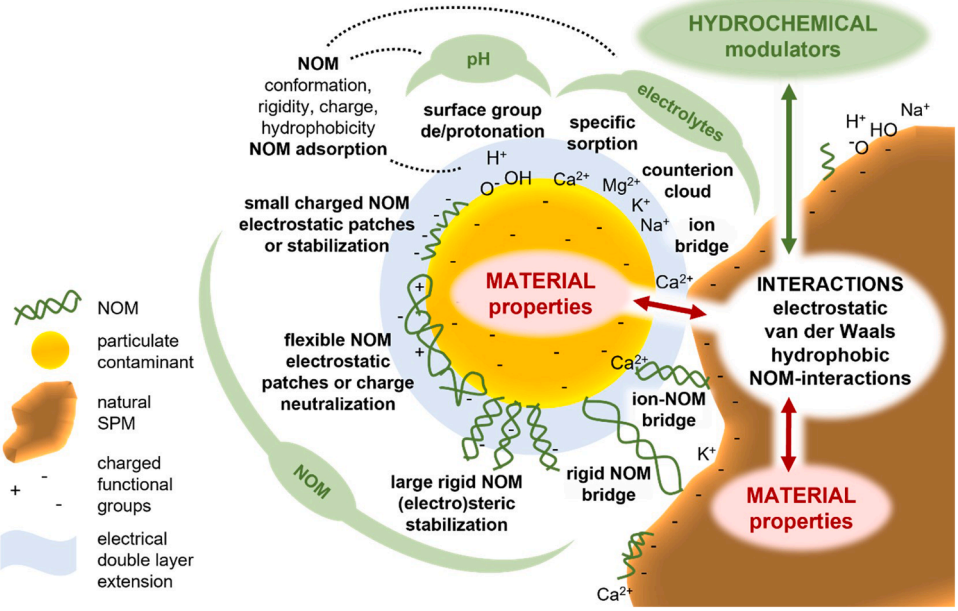

Fig. 1. Material-dependent interaction forces between SPM and particulate contaminants as modulated by hydrochemistry.

analogues that represent those characteristics of natural riverine SPM which are most relevant for heteroagglomeration. Analogues should reflect the complex composition/structure of natural SPM, as well as its heterogeneity in physicochemical surface properties, while comprising only few components to allow for reproducible generation. Our component selection is based on an extensive literature review (Walch et al., 2022), looking at the mineralogical and organic composition of natural riverine SPM and crucial components governing the dynamics of SPM formation. Selected minerals comprise illite, quartz, and hematite; and the amino acid tryptophan was chosen as a proxy substance to mimic some properties of microbial EPS (based on screening tests S2). Illite and quartz are representatives for the most abundant mineral constituents of natural riverine SPM, and hematite for minor but functionally important iron oxide and (oxy)hydroxide minerals (FeOx). Similarly, microbial EPS are mostly less abundant in SPM than refractory humic-like substances, but due to their heterogeneous properties, EPS are considered more relevant for flocculation. Being combined in realistic mass-ratios, the selected components not only reflect the composition of natural SPM, but also add to an increased heterogeneity in physicochemical surface properties, which is probably the most relevant feature of natural SPM when it comes to interactions with particulate contaminants.

The aim of this study was to develop and test reproducible SPM analogue flocs. We show that, using illite, quartz, hematite, and tryptophan in realistic mass-ratios, it is possible to generate complex SPM analogues, which are consistent regarding floc size and fractal dimension, and exhibit the desired robustness towards physical impacts and hydrochemical changes to allow proper handling in experimental setups.

2. Materials and methods

2.1. Hydrochemical Background

Following OECD test guideline No. 318 (OECD, 2017), hydrochemical test conditions comprised a pH range of 5–8.5, Suwannee River NOM (SR-NOM) at 0.1–10 ppmC and 0.1–10 mM $CaCl_2$ and $MgSO_4$ at a molar ratio of Ca:Mg 4:1 (hereafter just referred to as electrolytes). $CaCl_2$ was used, instead of $CaNO_3$ suggested by the guideline's *alternative medium*, because Cl^- is more abundant in river waters than NO_3^- (Salminen et al., 2005). SR-NOM stock was prepared according to the guideline: SR-NOM powder (2R101N, International Humic Substances Society) was dissolved in ultrapure water at pH 8 while agitating (> 16 h). After readjusting the pH and filtering the solution (sterile 0.2 μm PES bottle-top filters, Nalgene), the non-purgeable organic carbon concentration was determined with a total organic carbon (TOC) analyzer (TOC-L CPH/CPN, Shimadzu), and with 40 ± 1.5%$_{wt}$ was close to the expected values of 42.6%$_{wt}$ (Perdue, 2012) or 46.2%$_{wt}$ (IHSS, 2020a). Electrolyte solutions were prepared from calcium chloride dihydrate (≥ 99%, Sigma Aldrich) and magnesium sulfate heptahydrate (≥ 99.5%, EMSURE, Merck) at 800 or 80 and 200 or 20 mM, respectively, to receive a 4:1 Ca:Mg molar ratio in 1:1 mixtures. Intended pH values were adjusted with 0.1 M NaOH or HCl and monitored during measurements. Only at pH 8.5 the value dropped and had to be readjusted/maintained by constant NaOH additions during measurements (<0.1% of the total sample volume).

2.2. SPM Analogue components

Details on illite and hematite stock preparation are given in the supporting information (S3-A and S3-B). Briefly, illite rock chips (IMt-2, Silver Hill, MT, USA, Clay Minerals Society), were milled, dispersed, Na-exchanged and washed in repeated centrifugation-resuspension cycles, before narrowing the size distribution by differential centrifugation. Hematite was prepared by forced hydrolysis according to Wang et al. (2008). Quartz powder (SiO_2 0.5 μm spheres, Alfa Aesar) was dispersed in ultrapure water (weigh-in 1.5 g L^{-1}) using an ultrasonic probe (40 min, 40 W, TT13 tip, Sonoplus 3200, Bandelin). Dispersion efficacy was confirmed by checking hydrodynamic diameters (Zetasizer Nano ZS, Malvern). Characterization of mineral suspensions comprised hydrodynamic diameters, zeta potentials, polydispersity indices, isoelectric point determination in different hydrochemical backgrounds, and scanning electron microscopy (SEM) imaging, as reported in S3-C. L-Tryptophan solution was prepared at a carbon concentration of 2 g L^{-1} based on the carbon mass fraction in tryptophan (64.7%), dissolving the powder (≥ 98%, Sigma Aldrich) in ultrapure water by overnight shaking. Carbon recoveries, determined on a TOC analyzer (see 2.1.), were 98 ± 4%. All stocks were stored in the dark at 4 °C. The stability of mineral stocks was evaluated checking hydrodynamic diameters and zeta potentials (Zetasizer Nano ZS, Malvern) before use. Hematite suspensions were stable for 6 months (Figure S3–1), illite and quartz can be stored for at least one year, with quartz requiring 15–20 min ultrasonic probe sonication before use after resting for more than a few days. Organic stocks were replaced every two months.

2.3. SPM Analogue generation

For SPM analogue flocculation and characterization, a batch setup consisting of two stirred batch reactors connected to a laser diffractometer (Mastersizer 2000, Malvern) was designed, where the sample was passed through the measurement cell in "freefall" (~ 6 mL s^{-1}) to avoid any change in floc size or fractal dimension, with a peristaltic pump closing the circuit between the two batch reactors (S4-A). SPM analogue composition (Table 1) was based on typical riverine SPM compositions (see S1 and (Walch et al., 2022)) and screening tests (S2) and refined within the Mastersizer setup (S4-B). Starting from quartz and illite in ultrapure water at pH 5 (to maintain the positive surface charge of hematite upon addition), dilutions of hematite, tryptophan, electrolyte and SR-NOM stocks were quickly added (<15 s) in this sequence to both stirred batches simultaneously, establishing the SPM component concentrations given in Table 1, as well as the targeted hydrochemical background concentrations in a final volume of 800 mL for each batch (for details see S4-C).

Two procedures to generate SPM analogues were followed. (1) *Association procedure*: preparation directly in the two stirred batches connected to the Mastersizer, where circulation through the system and measurement of the sample were started right before the addition of hematite, tryptophan, electrolytes and SR-NOM, which allowed investigating the flocculation process. (2) *Shaker equilibration*: components were added into two magnetically stirred bottles (1 L centrifuge bottles, Heraeus) and then left on an overhead shaker for 1–24 h (16 rpm, Reax 20, Heidolph), before introducing the suspension into the Mastersizer setup for characterization.

2.4. SPM Analogue protocol validation

Hydrochemical conditions employed for protocol validation were 0.1 mM electrolytes at pH 5, without SR-NOM addition (for reasoning see S5-A). The *association procedure* was repeated 4 times using the same component stocks for within-batch reproducibility, and 3 times employing different component-stock batches for between-batches reproducibility. The *shaker equilibration* was validated only within-

Table 1
SPM analogue component fractions and final concentrations.

		Mass fractions [%$_{wt}$]	Conc. [mg L^{-1}]
Illite:Quartz Ratio 55:45	Quartz	41.85	18.83
	Illite	51.15	23.02
Hematite		7	3.15
Total mineral		*100*	*45*
Tryptophan (C-based)		+5% to minerals	2.25

batch (4 replicates). To test storability, SPM was prepared by *shaker equilibration* (shaken for 1 h) and stored in the dark fridge at 4 °C. Three batches were repeatedly resuspended at increasing time intervals (1 h, 1, 4, 8, 20 and 48 d), by three different means: overhead shaking (1 h, 16 rpm, Reax 20, Heidolph), ultrasonic bath sonication (20 min) and ultrasonic probe sonication (10 min, 40 W, TT13 tip, Sonoplus 3200, Bandelin) applied to each storage bottle containing 800 mL. Four additional parallel batches were resuspended by overhead shaking after 0, 5, 9 and 15 days of storage, respectively, to investigate storability without interim resuspension. Robustness towards changes in SPM concentration and stirring speed was tested by halving the concentration (from 45 to 22.5 ppm) and by varying the stirring speed between 50, 100 and 150 rpm, both, during SPM association, and after storage and resuspension.

SPM analogue reproducibility, storability and robustness were evaluated regarding stability and resilience of floc size and fractal dimension by means of laser diffractometry (Mastersizer 2000, Malvern). The fractal dimension describes the structural compactness of an agglomerate and takes values between 1 and 3, with 3 describing a solid sphere. We employ the fractal dimension for relative comparisons; absolute values might differ, as a mix of minerals at different concentrations with different refractive indices, particle sizes and shapes is considered, and all these properties impact the light scattering behavior. Volume-based median diameters ($d_{V0.5}$) and mass fractal dimensions (D_f) were recorded and plotted in a time-resolved manner. Volume-based size distributions and mode diameters (mode d_V) were employed to compare samples at a specific time point. Details are given in S5-B. Additionally, SPM analogue floc morphology was investigated by SEM imaging, as described in S3-C.

2.5. SPM analogues in changing hydrochemistry

The formation of SPM analogues in varying hydrochemical backgrounds was evaluated regarding floc size and fractal dimension in the Mastersizer setup after overnight *shaker equilibration*. Electrolyte (0.1, 1, 10 mM) and SR-NOM concentrations (0, 0.1, 1, 10 ppmC) were varied at pH 5, and zeta potentials were measured according to S3-C. The impact of pH (values 5, 7, 8.5) was investigated in batches prepared at 0.1 mM electrolytes without any SR-NOM, and at 10 mM with 1 ppmC SR-NOM. Adjustments of pH were done during SPM preparation, before overnight shaking, and continuously during measurement.

To evaluate whether flocs keep their integrity when hydrochemistry is changed after floc formation, and may be transferred into different hydrochemistries, SPM was generated at pH 5 without any electrolytes or SR-NOM added (SPMzero). After association, the hydrochemistry was adjusted by adding diluted electrolyte and SR-NOM stocks to reach a hydrochemical background of 0.1 mM and 1 ppmC, while halving the SPM concentration to 22.5 ppm.

3. Results and discussion

3.1. Complex Near-Natural spm analogue flocs can be reproducibly prepared

Flocs formed within minutes with diameters consistently around 7 μm and fractal dimensions slightly above 2.5. Signals in the size range of the individual components were not recorded by the Mastersizer 2000. The generated flocs can be considered *primary flocs*, characterized by rather small floc sizes and compact structures (indicated by high fractal dimensions). Primary flocs constitute base units that can assemble to larger more loose *secondary flocs*, increasingly colonized by microorganisms. Within a recent floc structure hierarchy (Spencer et al., 2021), *microflocs* and *particle-particle associations (flocculi)* would be the corresponding classes. Considering structural floc dynamics throughout the year (Zimmermann-Timm, 2002), type 3 (densely packed mineral particles and detritus < 150 μm, often spherical) which is typical in winter, autumn, and during flood, would correspond.

The individual component preparations were highly consistent (Table S3–1), meeting the criteria to allow a reproducible SPM analogue generation, which was confirmed regarding floc size and fractal dimension, whether the same (Figure S6–1) or different component batches (Fig. 2) were employed. After an initial floc association phase, the diameter and fractal dimension reached an interim plateau. Size distributions were stable during that time, narrow and consistent between replicates (Fig. 2b, Figure S6–1 b). The relative standard deviations (RSDs) of the volume-based mode diameters (mode d_V) compared after 1 h were 4.8% (mode d_V= 7.3 μm, n = 4) and 6.7% (mode d_V = 7.9 μm, n = 3), for within-batch and between-batches replicates (see 2.4.) respectively. The size of the flocs falls within the range of natural riverine floc sizes covering < 1 to 1000 μm (Zimmermann-Timm, 2002), with typical values from few μm up to (few) hundred μm (Guo and He, 2011; Lartiges et al., 2001; Woodward and Walling, 2007). Fractal dimensions exhibited values within the predetermined range for shear flow (i.e., ≥ 2.4) (Conchuir et al., 2014), with RSDs of 0.9% (D_f = 2.56, n = 4) within-batch, and 5.1% (D_f = 2.7, n = 3) between batches. These quite high fractal dimensions partly result from the way laser scattering data were fit (see S5-B), however, the optimization of the floc composition to yield stable, robust flocs, probably also entailed compact structures.

SPM analogue preparation by 24 h *shaker equilibration* was also well reproducible (Fig. 3a), exhibiting within-batch RSDs (n = 4, compared at 60 min) of 11.1% and 1.4%, for size (mode d_V = 6.6 μm) and fractal dimension (D_f = 2.65) respectively. Both parameters were similar to freshly associated flocs compared at 60 min (Fig. 3b). For size distributions see Figure S6–2.

SEM images (Fig. 4a) show complex SPM analogue floc structures that incorporate all constituents, generating heterogeneous surfaces. Images resemble those of natural SPM (Buffle et al., 1998; Le Meur et al., 2016; Slomberg et al., 2016; Wheatland et al., 2017). With hematite being the smallest and quartz the largest component (Fig. 4b), their relative sizes reflect trends observed for natural SPM, where quartz-shares increase in the larger size fraction and FeOx mainly form nanoparticles or patchy coatings on larger particles (Walch et al., 2022). As expected from the positive surface charge of hematite (Figure S3–2) in the given hydrochemistry (pH 5, 0.1 mM electrolytes, no SR-NOM), SEM images show hematite to act as bridging-agent between illite and quartz (Figure S6–3). Hematite mainly distributes on the negative edges of illite (Figure S6–4), where it is likely associated with tryptophan, as NOM-FeOx associations seaming clay edges have been previously reported (Poulton and Raiswell, 2005). Quartz mostly distributes on the floc surface, while the core is composed of illite-hematite associations (Figure S6–5). This reflects modeling results (Frungieri et al., 2020) which showed that agglomeration of imbalanced mixtures of positively and negatively charged particles depleted minority particles first, while majority particles cover the agglomerate surface. In our case, positive surface charges (on hematite and illite edges) represent the minority and negative charges (on quartz and illite basal planes) the majority, as confirmed by an overall negative floc zeta potential of -18 ± 1.2 mV.

3.2. Floc Size evolution is controlled by particle concentration and stirring speed

Floc association and size evolution proceeds in three phases: (1) quick, diffusion-limited association governed by electrostatic forces, (2) a shear and concentration dependent restructuring and compaction phase, (3) further floc growth approaching a flocculation-rupture regime.

Initial association is fueled by a high primary particle number allowing for a high collision frequency. Due to opposite charges of the components (Figure S3–2) in the present hydrochemistry (pH 5, 0.1 mM electrolytes), association is probably diffusion limited (attachment efficiency α ~ 1) and attachment governed by electrostatic attractions

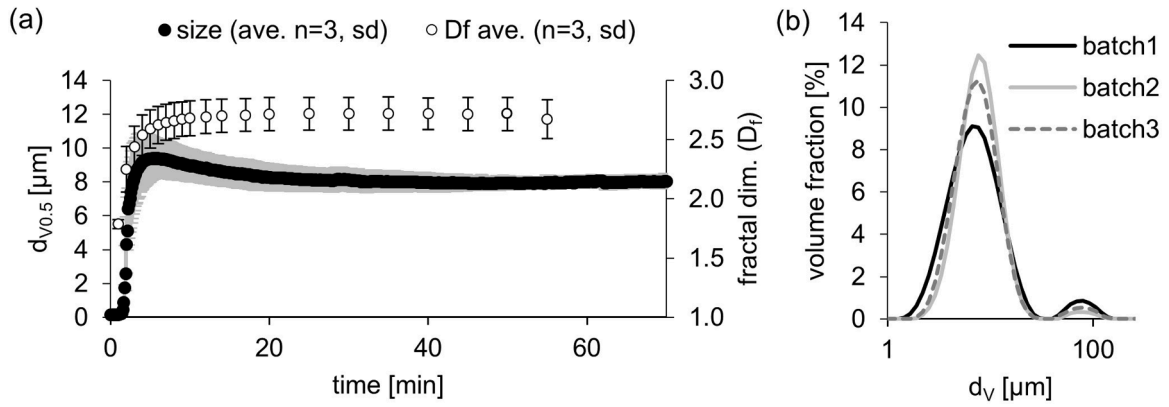

Fig. 2. (a) Evolution of volume-based median floc diameters ($d_{V0.5}$) and fractal dimensions (D_f) of three between-batches replicates (ave. ± sd) during floc association (pH 5, 0.1 mM electrolytes); (b) respective size distributions at 60 min.

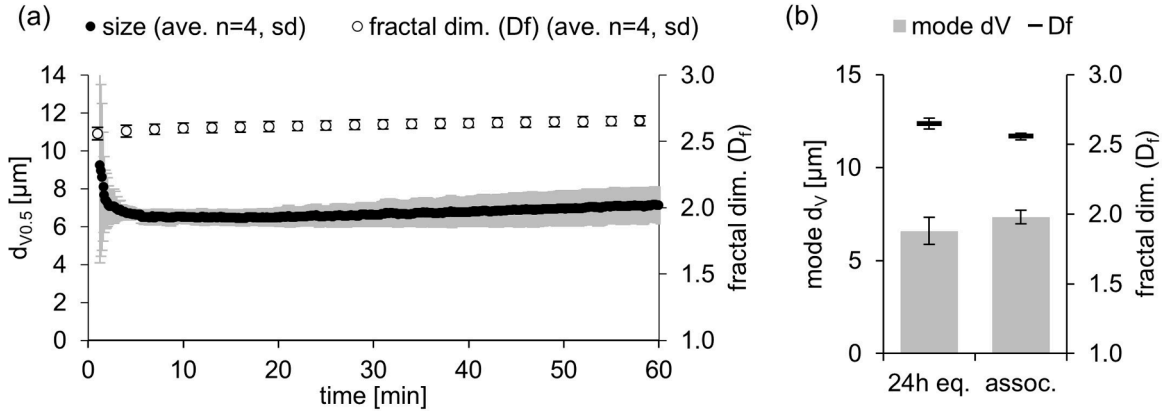

Fig. 3. (a) Volume-based median floc diameters ($d_{V0.5}$) and fractal dimensions (D_f) of four within-batch replicates (ave. ± sd) prepared by 24 h *shaker equilibration*; (b) Volume-based mode diameters (d_V) and fractal dimensions of four within-batch replicates (ave. ± sd) prepared by *association* and *shaker equilibration* methods (compared at 60 min measurement time).

(neutralization of negative charges on illite and quartz by addition of positive hematite, $Ca^{2+}$and Mg^{2+}). The dominance of electrochemical mechanisms in primary floc formation was also inferred from 3D structural observations of natural flocs (Spencer et al., 2021). Collision-dependance is confirmed by a slower and slightly retarded association at halved concentrations (Fig. 5a). Lower stirring should also reduce collisions but had little impact on the early association phase. This is because the collision rate is proportional to the concentration squared, while proportional to the mean shear rate (Tran et al., 2018). Additionally, all primary particles (quartz, illite, hematite) were nano-sized, and diffusion-driven collisions prevail over orthokinetic (advection-driven) collisions (Figure S7–1 a), resulting in an insignificance of shear (Han and Lawler, 1992; Praetorius et al., 2020).

With a decreasing primary particle number, the collision frequency decreases, while, simultaneously, charge heterogeneities are neutralized, letting floc size plateau. According to the model by Frungieri et al. (2020), size stabilizes when minority particles (in terms of surface charge) are used up and floc surfaces are covered by majority particles, establishing an electrostatic energy barrier. The model showed good stabilization at 85% majority particles, while growth was self-accelerating at equal shares. A rough calculation of the positive and negative surface areas in the present SPM component mix yields 92.5% negative and 7.5% positive surface (Table S7–1). Since the composition was based on natural SPM composition, future research should address if natural flocs require a certain composition ratio to persist as stable flocs.

At 45 ppm SPM, size peaked and slightly decreased before plateauing (Fig. 5a). Size reduction was suggested to result from floc compaction and restructuring (Selomulya et al., 2003), which is supported by observations of an increase in floc circularity during that phase (Vlieghe et al., 2014). A zoom into the fractal dimension axis (Fig. 5b) reveals that size peaks and dips before D_f reaches its maximum, and D_f continues to slowly increase (indicating compaction) until the floc size plateaus. Restructuring can proceed in two ways: (1) As a consequence of charge neutralization, the attachment efficiency has dropped, and collision energy is dissipated by slowly continued compaction rather than flocculation; (2) Flocs have reached a size-range where shear forces start to act on them and induce restructuring, which was demonstrated by a model by Becker et al. (2009). Since, in the case of halved SPM concentrations, a size peak-dip sequence was not observed, a ballistic effect is more likely than a shear effect.

At some point flocs resume growth (see size at 50 rpm in Fig. 5a) for two possible reasons: (1) floc restructuring reduces the suggested surface enrichment of (negatively charged) majority particles (Frungieri et al., 2020), lowering the electrostatic energy barrier; (2) compaction increases the components' coordination number and floc stability (Conchuir et al., 2014; Selomulya et al., 2003), inhibiting dissipation of collision energy by deformation, and allowing energy barriers to be overcome. When flocculation is resumed, D_f slowly decreases again (see D_f at 50 rpm in Fig. 5b). This coincides with the clear proliferation of a second peak in the size distribution (Figure S7–2), confirming that primary SPM flocs flocculate to larger, again less compact secondary flocs, which finally approach a flocculation-rupture regime (see size at 50 rpm in Fig. 5a) due to shear-induced rupture of loose flocs (Becker et al., 2009).

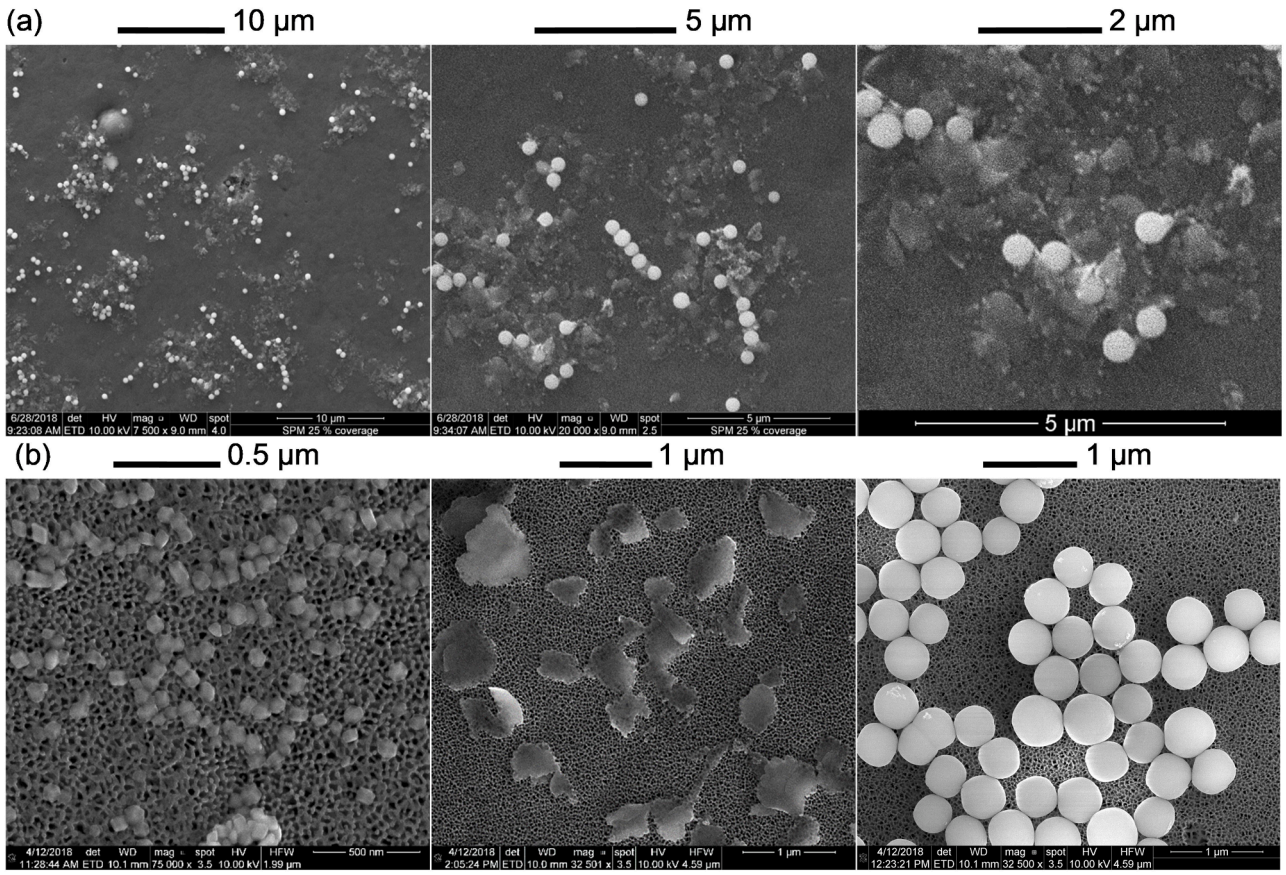

Fig. 4. SEM images (a) of the SPM analogue flocs at different resolutions and (b) of the mineral constituents: hematite, illite and quartz (from left to right).

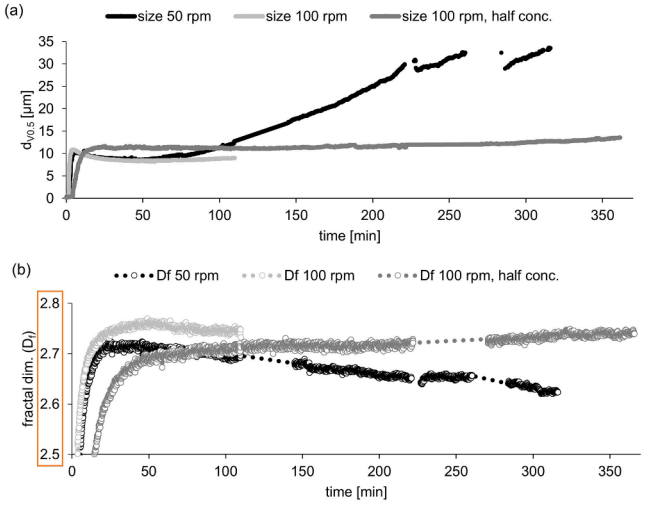

Fig. 5. Co-evolution of (a) SPM analogue floc size and (b) fractal dimension (note the axis zoom), as controlled by stirring speed (shear forces) and SPM concentration.

The extension of the interim size-plateau was clearly shorter at reduced stirring speed (50 instead of 100 rpm) (Fig. 5a). As SPM flocs have reached several µm in size, orthokinetic (advective) collisions dominate (Figure S7–1 b). Lower stirring speed lowers the approach velocity of flocs and thus their mutual repulsion by hydrodynamic effects (Gregory, 2005). As flocs are fractal agglomerates, not solid spheres, a less turbulent flow allows permeation of flocs and induces a transition from curvilinear towards rectilinear floc trajectories, which increases the collision frequency (Bäbler et al., 2006; Han and Lawler, 1992; Li and Logan, 1997; Veerapaneni and Wiesner, 1996). Lower shear stress and lower ballistic stress (Tran et al., 2018) additionally reduce floc rupture and allow for quicker resumption of growth. Halving the concentrations (22.5 instead of 45 ppm SPM) at 100 rpm stirring prolonged the plateauing phase (Fig. 5a), as explained by a reduced collision frequency slowing down compaction and the onset of further floc growth, together with relatively high shear forces sustaining floc rupture and/or hydrodynamic effects – i.e., curvilinearity of collision trajectories.

3.3. SPM Analogues are storable, resilient and robust upon resuspension

Storage and resuspension tests revealed that flocs can be stored for at least 8 d without any significant change in fractal dimension, volume-based diameter (Fig. 6), or size distribution (Figure S8–1), no matter if batches were repeatedly resuspended or stored for a certain time without interim resuspension (parallel batches). The different resuspension techniques applied had no impact on floc size after a stabilization time of 60 min (Fig. 6a), while the fractal dimension was generally lower for sonication treatments. The latter reflects observations of partial floc rupture through sonication, and regrowth within the stabilization time. Shaker-resuspended samples, in turn, exhibited breakage of initial larger clusters to original floc size when introduced into the stirred batch system. Within-treatment RSDs over 8 or 9 storage days ranged from 0.9% to 1.4% for D_f and from 4% (ultrasonic probe) via 5.5% (shaker) to 13% (ultrasonic bath) for size ($d_{V0.5}$). At 15 or 20 days of storage, deviations of $d_{V0.5}$ and D_f (Fig. 6) as well as size distributions (Figure S8–1) were clearly pronounced for shaker-resuspension. Employing ultrasound, storability may be extended beyond 8 days, close to 20 days.

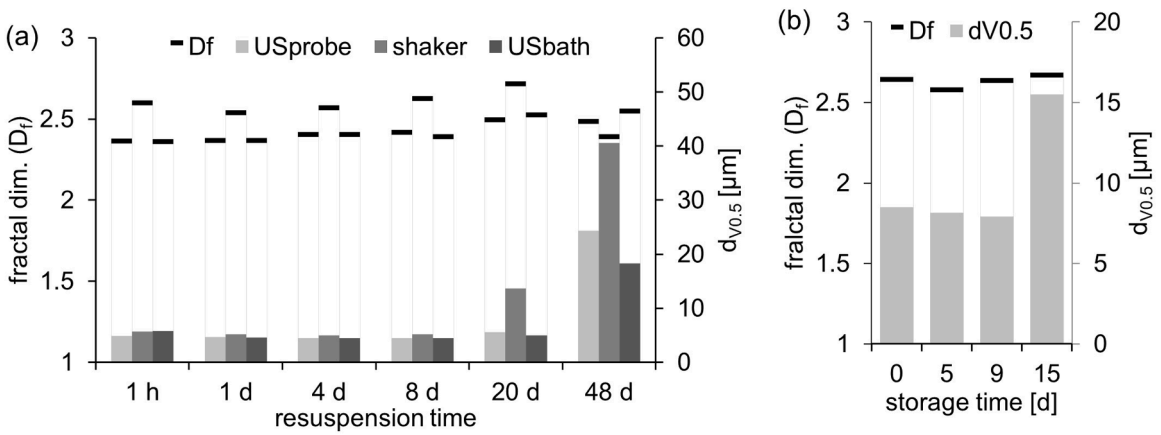

Fig. 6. Volume-based median diameter and fractal dimension (D_f) at 60 min measurement time, after resuspension (a) of the same three batches at different time intervals by a different treatment each; (b) of independent batches resuspended by shaking for 1 h after different storage times each.

Varying stirring speeds (between 50, 100 & 150 rpm) after resuspension (by ultrasonic probe), hardly influenced the volume-based median SPM floc diameter. The RSD of floc size among speeds (compared after 60 min of stirring) was only 7%, which confirms results of Yu et al. (Yu et al., 2011) showing that, after floc breakage and regrowth, shear conditions had little impact on size. The concentration effect on floc size was also concealed by resuspension. During floc association, halved SPM concentration (22.5 ppm) yielded a higher plateau size (mode d_V = 11.1 µm) than 45 ppm (mode d_V= 7.3 µm) (Figure S8–2 a). After resuspension, batches prepared at 22.5 and 45 ppm, as well as 45 ppm batches diluted 1:1 (either before, or after 24 h shaking) all approached similar floc sizes when exposed to controlled stirring conditions (100 rpm) in the Mastersizer setup for about 1.5 h (mode d_V = 9.1 - 10.4 µm) (Figure S8–2 b).

3.4. SPM Formation, size and fractal dimension depend on hydrochemistry

When being prepared in the respective target hydrochemistry, not all combinations of electrolyte and SR-NOM concentrations led to floc formation (Fig. 7a). This can be explained by electrostatic stabilization through NOM: SR-NOM is dominated by hydrophobic acids (66–70% of the carbon mass) (Ratpukdi et al., 2009), which are rich in carboxyl groups (IHSS, 2020b; Schumacher et al., 2006). The latter exhibit a low pK_a, making SR-NOM highly negatively charged.

Electrolytes counteracted NOM-stabilization, and the more SR-NOM was present, the more electrolytes were required to induce flocculation (Fig. 7a). Electrolytes act in several ways: sorption of counterions and strong electrical double layer compression destabilize suspensions (Gregory, 2005), and multivalent ions (especially Ca^{2+}) may induce interparticle bridging (Wang et al., 2017) or bridging flocculation involving NOM (Philippe and Schaumann, 2014) (Fig. 1). Combinations of 0.1 mM electrolytes with 0.1 and 1 ppmC SR-NOM, and 1 mM electrolytes with 0.1 ppmC SR-NOM yielded no flocs. This allows to predict that even higher (10 ppmC) SR-NOM concentrations would as well prohibit floc formation at 0.1 mM and 1 mM electrolytes.

Regarding floc size, combined effects of SR-NOM and electrolyte concentrations were not linear. A smaller size of flocs at 10 mM electrolytes with 1 ppmC than with 10 ppmC SR-NOM (Figure 7 a), for example, may either indicate that Ca^{2+}-induced bridging flocculation is limited by SR-NOM concentrations, or that at higher electrolyte concentrations, SO_4^{2-} competes with SR-NOM for sorption sites on hematite (Gu et al., 1995; Tan and Kilduff, 2007). The latter is likely, as both, high electrolytes and SR-NOM strongly reduced or inversed the positive surface charge of hematite (Figure S3–2). An effect of SO_4^{2-} is also supported by a slightly decreasing D_f (from 2.86 down to 2.56) with increasing electrolyte concentrations (Figure 7 a). Of the tested combinations, the largest flocs (at pH 5) resulted at 0.1 ppmC SR-NOM and 1 mM electrolytes (Fig. 7a), concentrations at which hematite was at its isoelectric point (for SR-NOM) or exhibited low positive charge (for electrolytes) (Figure S3–2). Generally, flocculation will be favored by an optimum ratio of SR-NOM, available (favorable) sorption sites, and sorption- or bridging-enhancing electrolyte ions. For mechanistic insights, further research is required.

An impact of pH was observed at low electrolyte concentrations (0.1 mM) and in the absence of SR-NOM (Fig. 7b). Floc compactness (D_f) decreased with increasing pH and finally resulted in smaller flocs (at pH 8.5), as explained by stronger electrostatic repulsion between SPM components at increasing pH, especially when hematite turns negative at pH 8.5 (Figure S3–2). In presence of 10 mM electrolytes and 1 ppmC

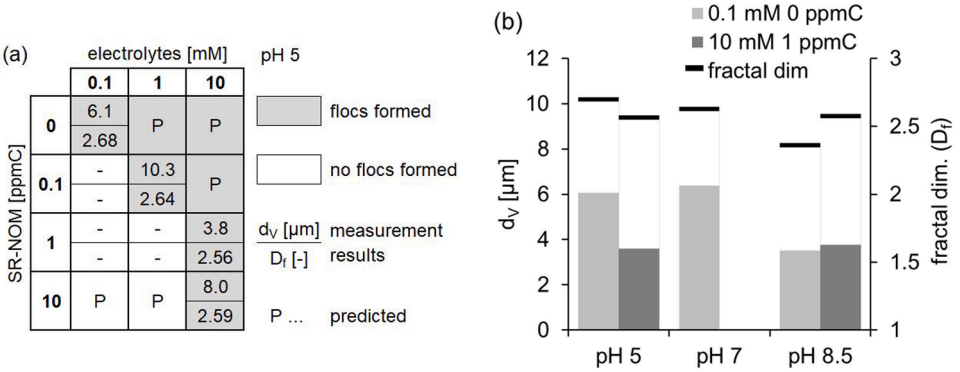

Fig. 7. (a) Floc formation by *shaker equilibration* in different hydrochemistries; and (b) impact of pH on SPM analogue floc size and fractal dimension.

SR-NOM, the pH-effect was probably masked by overriding impacts of electrolytes and SR-NOM (Fig. 7b).

3.5. SPM Analogues remain stable upon transfer into unfavorable hydrochemistries

As flocculation was prohibited by some hydrochemical conditions, SPM analogues were generated without any electrolyte or SR-NOM addition (SPMzero) and adjusted to target hydrochemistries unfavorable for flocculation. SPMzero association at pH 5 (positive charge of hematite) yielded a larger plateau floc size at 60 min (mode d_V= 15.42 ± 0.96 µm, within-batch), than flocs associated at 0.1 mM electrolytes (mode d_V= 7.3 ± 0.4 µm), in accordance with hematite being more positively charged in absence of electrolytes (Figure S3–2).

The modification of hydrochemistry to 0.1 mM electrolytes & 1 ppmC SR-NOM in course of a 1:1 dilution of both, freshly associated and overnight shaker-equilibrated SPMzero, did not induce disintegration of flocs (Figures S8–3 and S8–4), even though these hydrochemical conditions prohibited flocculation (Fig. 7a). Agglomeration is frequently reported to not be fully reversible and de-agglomeration by unfavorable hydrochemistry produces fragments rather than single particles (Baalousha, 2009; Loosli et al., 2013; Mohd Omar et al., 2014), as probably mainly weak bonds (secondary minima) are broken (Philippe and Schaumann, 2014; Wang et al., 2016). Still, the extent of de-agglomeration was found to increase with concentration of stabilizing NOM and with reaction time, as molecules slowly migrate into agglomerates (Baalousha et al., 2009; Loosli et al., 2013). However, even after storage for 6 d and resuspension (by shaking over night for >18 h), SPMzero floc integrity was not affected by the modified hydrochemistry and resuspended flocs approached the sizes of freshly hydrochemistry-adjusted flocs after about 1.5 h in controlled stirring conditions (Figures S8–3 and S8–4). Consequently, after every physical or chemical impact, a conditioning phase in the final experimental stirring conditions should be allowed.

4. Conclusions

In this study we developed SPM analogues which can be used to investigate interactions of SPM with particulate contaminants, such as engineered nanomaterials, nano- and microplastics, soot, or others, at environmentally relevant freshwater conditions. Natural SPM composition is complex and characterized by heterogeneous physicochemical surface properties. Hence, interactions of contaminant particles with SPM will be governed by multiple co-occurring interaction mechanisms, which are even more tortuous considering naturally occurring hydrochemistries. While simple test systems are highly important to gain in-depth mechanistic understanding, complexity cannot be neglected when trying to properly represent natural systems and informed simplifications should guide the development of environmentally relevant and standardizable test systems.

Our SPM analogues were designed to represent those physicochemical surface properties of natural SPM relevant for interactions with particulate contaminants. Selected components not only represent the most abundant components of natural riverine SPM in realistic mass-ratios, but also maximize heterogeneity in physicochemical surface properties, and the resultant SPM analogue flocs reflect the complex composition and structure of natural riverine SPM. These analogues could be reproducibly generated at different agitation conditions (shaking, stirring), as association is controlled by surface chemistry.

The primary role of surface chemistry for flocculation was confirmed by inhibition when component surfaces are repulsive in hydrochemistries unfavorable for floc formation. However, flocs associated under favorable conditions did not disintegrate upon subjection to hydrochemistries suppressing flocculation and SPM analogues can be transferred into unfavorable hydrochemistries for follow-up experiments.

For direct use of freshly associated flocs in experiments, the experiment duration should not exceed the extent of the stable size plateau, which depends on shear forces and SPM concentrations in the system. For flocculation conditions tested here, the plateauing phase lasted for at least 1.5 h. While floc association was somewhat sensitive to varying stirring speeds and SPM concentrations, analogues which had sedimented and rested during storage exhibited extended stability and higher robustness to modified stirring speeds and SPM concentrations upon resuspension.

Physical or chemical impacts, such as changed agitation (stirring or shaking), sedimentation and storage, resuspension (by shaking, ultrasonic bath or probe), dilution, or changed hydrochemistry, induced elastic changes, and the SPM flocs returned to a stable size when exposed to controlled stirring for 1 - 1.5 h. The resilience of SPM analogues to sedimentation and resuspension and the storability for at least 8 days eases handling in the lab and allows for flexibility when planning experiments. The flocs also seem to be quite robust to varying stirring speeds. However, if a different agitation regime is employed, stability of size should be reevaluated and may be tuned via stirring speed and SPM concentration.

The presented SPM analogues constitute the missing link between complex natural systems and simplistic approaches, providing the prerequisite for the development of standardizable and yet environmentally relevant experimental protocols to assess the behavior and fate of particulate contaminants in the presence of SPM. Employing these analogues, fate processes like heteroagglomeration (OECD, 2020), SPM-assisted transport or sedimentation, bioavailability and uptake in the presence of SPM may be investigated in a comparable manner for various types of particulate contaminants.

Funding sources

This work was supported by EU Horizon 2020 project NanoFASE [grant number 646002].

CRediT authorship contribution statement

Helene Walch: Conceptualization, Methodology, Validation, Formal analysis, Investigation, Writing – original draft, Visualization, Project administration. **Antonia Praetorius:** Conceptualization, Methodology, Writing – review & editing, Supervision. **Frank von der Kammer:** Conceptualization, Methodology, Writing – review & editing, Supervision, Funding acquisition. **Thilo Hofmann:** Resources, Writing – review & editing, Supervision.

Declaration of Competing Interest

The authors declare no competing financial interest.

Data availability

Data will be made available on request.

Acknowledgments

We sincerely thank Nathalie Tepe, Vesna Micic Batka and Gerlinde Habler for SEM imaging. Financial support from the EU Horizon 2020 project NanoFASE [grant number 646002] is gratefully acknowledged.

Supplementary materials

Supplementary material associated with this article can be found, in the online version, at doi:10.1016/j.watres.2022.119385.

References

Abdolahpur Monikh, F., Praetorius, A., Schmid, A., Kozin, P., Meisterjahn, B., Makarova, E., Hofmann, T., von der Kammer, F., 2018. Scientific rationale for the development of an OECD test guideline on engineered nanomaterial stability. NanoImpact 11, 42–50. https://doi.org/10.1016/j.impact.2018.01.003.

Adam, V., Loyaux-Lawniczak, S., Labille, J., Galindo, C., del Nero, M., Gangloff, S., Weber, T., Quaranta, G., 2016. Aggregation behaviour of TiO2 nanoparticles in natural river water. J. Nanoparticle Res. 18, 13. https://doi.org/10.1007/s11051-015-3319-4.

Baalousha, M., 2009. Aggregation and disaggregation of iron oxide nanoparticles: influence of particle concentration, pH and natural organic matter. Sci. Total Environ. 407, 2093–2101. https://doi.org/10.1016/j.scitotenv.2008.11.022.

Baalousha, M., Lead, J.R., Von Der Kammer, F., Hofmann, T., 2009. Natural Colloids and Nanoparticles in Aquatic and Terrestrial Environments, in: environmental and Human Health Impacts of Nanotechnology. John Wiley & Sons, Ltd, pp. 109–161. https://doi.org/10.1002/9781444307504.ch4.

Bäbler, M.U., Sefcik, J., Morbidelli, M., Bałdyga, J., 2006. Hydrodynamic interactions and orthokinetic collisions of porous aggregates in the Stokes regime. Phys. Fluid. 18, 013302 https://doi.org/10.1063/1.2166125.

Baun, A., Sayre, P., Steinhäuser, K.G., Rose, J., 2017. Regulatory relevant and reliable methods and data for determining the environmental fate of manufactured nanomaterials. NanoImpact 8, 1–10. https://doi.org/10.1016/j.impact.2017.06.004.

Becker, V., Schlauch, E., Behr, M., Briesen, H., 2009. Restructuring of colloidal aggregates in shear flows and limitations of the free-draining approximation. J. Colloid Interface Sci. 339, 362–372. https://doi.org/10.1016/j.jcis.2009.07.022.

Buffle, J., Wilkinson, K.J., Stoll, S., Filella, M., Zhang, J., 1998. A generalized description of aquatic colloidal interactions: the three-colloidal component approach. Environ. Sci. Technol. 32, 2887–2899. https://doi.org/10.1021/es980217h.

Conchuir, B.O., Harshe, Y.M., Lattuada, M., Zaccone, A., 2014. Analytical model of fractal aggregate stability and restructuring in shear flows. Ind. Eng. Chem. Res. 53, 9109–9119. https://doi.org/10.1021/ie4032605.

Dale, A.L., Lowry, G.V., Casman, E.A., 2015. Much ado about α: reframing the debate over appropriate fate descriptors in nanoparticle environmental risk modeling. Environ. Sci. Nano 2, 27–32. https://doi.org/10.1039/c4en00170b.

Droppo, I.G., 2001. Rethinking what constitutes suspended sediment. Hydrol. Process. 15, 1551–1564. https://doi.org/10.1002/hyp.228.

Eisma, D., 1993. Suspended Matter in the Aquatic Environment. Springer Berlin Heidelberg, Berlin, Heidelberg. https://doi.org/10.1007/978-3-642-77722-6.

Elimelech, M., Gregory, J., Jia, X., Williams, R.A., 1995. Modelling of aggregation processes. Particle Deposition & Aggregation. Elsevier, Woburn, pp. 157–202. https://doi.org/10.1016/B978-075067024-1/50006-6.

Frungieri, G., Babler, M.U., Vanni, M., 2020. Shear-induced heteroaggregation of oppositely charged colloidal particles. Langmuir 36, 10739–10749. https://doi.org/10.1021/acs.langmuir.0c01536.

Gallego-Urrea, J.A., Hammes, J., Cornelis, G., Hassellöv, M., 2016. Coagulation and sedimentation of gold nanoparticles and illite in model natural waters: influence of initial particle concentration. NanoImpact 3–4, 67–74. https://doi.org/10.1016/j.impact.2016.10.004.

Geitner, N.K., Marinakos, S.M., Guo, C., O'Brien, N., Wiesner, M.R., 2016. Nanoparticle surface affinity as a predictor of trophic transfer. Environ. Sci. Technol. 50, 6663–6669. https://doi.org/10.1021/acs.est.6b00056.

Gregory, J., 2005. Particles in Water. CRC Press, Boca Raton. https://doi.org/10.1201/9780203508459.

Gu, B., Schmitt, J., Chen, Z., Liang, L., McCarthy, J.F., 1995. Adsorption and desorption of different organic matter fractions on iron oxide. Geochim. Cosmochim. Acta 59, 219–229. https://doi.org/10.1016/0016-7037(94)00282-Q.

Guo, L., He, Q., 2011. Freshwater flocculation of suspended sediments in the Yangtze River. China. Ocean Dyn. 61, 371–386. https://doi.org/10.1007/s10236-011-0391-x.

Han, M., Lawler, D.F., 1992. The (Relative) insignificance of G in flocculation. J. Am. Water Works Assoc. 84, 79–91. https://doi.org/10.1002/j.1551-8833.1992.tb05869.x.

Henning, K.-.H., Damke, H., Kasbohm, J., Puff, T., Breitenbach, E., Theel, O., Kießling, A., 2001. Schwebstoffbeschaffenheit im Odersystem. Greifswald.

Hofmann, T., von der Kammer, F., 2009. Estimating the relevance of engineered carbonaceous nanoparticle facilitated transport of hydrophobic organic contaminants in porous media. Environ. Pollut. 157, 1117–1126. https://doi.org/10.1016/j.envpol.2008.10.022.

IHSS, 2020a. Elemental Compositions and Stable Isotopic Ratios of IHSS Samples [WWW Document]. URL http://humic-substances.org/elemental-compositions-and-stable-isotopic-ratios-of-ihss-samples/ (last accessed on 23.11.2022).

IHSS, 2020b. Acidic Functional Groups of IHSS Samples [WWW Document]. URL http://humic-substances.org/acidic-functional-groups-of-ihss-samples/ (last accessed on 23.11.2022).

Labille, J., Harns, C., Bottero, J.-.Y., Brant, J., 2015. Heteroaggregation of titanium dioxide nanoparticles with natural clay colloids. Environ. Sci. Technol. 49, 6608–6616. https://doi.org/10.1021/acs.est.5b00357.

Lartiges, B.S., Deneux-Mustin, S., Villemin, G., Mustin, C., Barrès, O., Chamerois, M., Gerard, B., Babut, M., 2001. Composition, structure and size distribution of suspended particulates from the Rhine River. Water Res. 35, 808–816. https://doi.org/10.1016/S0043-1354(00)00293-1.

Le Meur, M., Montargès-Pelletier, E., Bauer, A., Gley, R., Migot, S., Barres, O., Delus, C., Villiéras, F., 2016. Characterization of suspended particulate matter in the Moselle River (Lorraine, France): evolution along the course of the river and in different hydrologic regimes. J. Soil. Sediment. 16, 1625–1642. https://doi.org/10.1007/s11368-015-1335-8.

Li, X., Logan, B.E., 1997. Collision frequencies between fractal aggregates and small particles in a turbulently sheared fluid. Environ. Sci. Technol. 31, 1237–1242. https://doi.org/10.1021/es960772o.

Li, Y., Wang, X., Fu, W., Xia, X., Liu, C., Min, J., Zhang, W., Crittenden, J.C., 2019. Interactions between nano/micro plastics and suspended sediment in water: implications on aggregation and settling. Water Res. 161, 486–495. https://doi.org/10.1016/j.watres.2019.06.018.

Loosli, F., Le Coustumer, P., Stoll, S., 2013. TiO2nanoparticles aggregation and disaggregation in presence of alginate and Suwannee River humic acids. pH and concentration effects on nanoparticle stability. Water Res. https://doi.org/10.1016/j.watres.2013.07.021.

Mohd Omar, F., Abdul Aziz, H., Stoll, S., 2014. Aggregation and disaggregation of ZnO nanoparticles: influence of pH and adsorption of Suwannee River humic acid. Sci. Total Environ. 468–469, 195–201. https://doi.org/10.1016/j.scitotenv.2013.08.044.

OECD, 2020. GD 318: guidance Document for the testing of dissolution and dispersion stability of nanomaterials and the use of the data for further environmental testing and assessment strategies. Series on Testing and Assessment No. 318. OECD Guidel. Test. Chem. 1–48.

OECD, 2017. Test No. 318: Dispersion Stability of Nanomaterials in Simulated Environmental Media, OECD Guidelines for the Testing of Chemicals, Section 3. OECD, Paris. https://doi.org/10.1787/9789264284142-en.

Oriekhova, O., Stoll, S., 2018. Heteroaggregation of nanoplastic particles in the presence of inorganic colloids and natural organic matter. Environ. Sci. Nano 5, 792–799. https://doi.org/10.1039/C7EN01119A.

Perdue, M., 2012. Replenishment of the Reference Suwannee River Natural Organic Matter (NOM). Muncie.

Philippe, A., Schaumann, G.E., 2014. Interactions of dissolved organic matter with natural and engineered inorganic colloids: a review. Environ. Sci. Technol. 48, 8946–8962. https://doi.org/10.1021/es502342r.

Poulton, S.W., Raiswell, R., 2005. Chemical and physical characteristics of iron oxides in riverine and glacial meltwater sediments. Chem. Geol. 218, 203–221. https://doi.org/10.1016/j.chemgeo.2005.01.007.

Praetorius, A., Badetti, E., Brunelli, A., Clavier, A., Gallego-Urrea, J.A., Gondikas, A., Hassellöv, M., Hofmann, T., Mackevica, A., Marcomini, A., Peijnenburg, W., Quik, J.T.K., Seijo, M., Stoll, S., Tepe, N., Walch, H., von der Kammer, F., 2020. Strategies for determining heteroaggregation attachment efficiencies of engineered nanoparticles in aquatic environments. Environ. Sci. Nano 7, 351–367. https://doi.org/10.1039/C9EN01016E.

Praetorius, A., Labille, J., Scheringer, M., Thill, A., Hungerbühler, K., Bottero, J.-.Y., 2014a. Heteroaggregation of titanium dioxide nanoparticles with model natural colloids under environmentally relevant conditions. Environ. Sci. Technol. 48, 10690–10698. https://doi.org/10.1021/es501655v.

Praetorius, A., Tufenkji, N., Goss, K.-.U., Scheringer, M., von der Kammer, F., Elimelech, M., 2014b. The road to nowhere: equilibrium partition coefficients for nanoparticles. Environ. Sci. Nano 1, 317–323. https://doi.org/10.1039/C4EN00043A.

Quik, J.T.K., Velzeboer, I., Wouterse, M., Koelmans, A.A., van de Meent, D., 2014. Heteroaggregation and sedimentation rates for nanomaterials in natural waters. Water Res. 48, 269–279. https://doi.org/10.1016/j.watres.2013.09.036.

Ratpukdi, T., Rice, J.A., Chilom, G., Bezbaruah, A., Khan, E., 2009. Rapid Fractionation of Natural Organic Matter in Water Using a Novel Solid-Phase Extraction Technique. Water Environ. Res. 81, 2299–2308. https://doi.org/10.2175/106143009x407302.

Salminen, R., Batista, M.J., Bidovec, M., Demetriades, A., De Vivo, B., De Vos, W., Duris, M., Gilucis, A., Gregorauskiene, V., Halamic, J., Heitzmann, P., Lima, A., Jordan, G., Klaver, G., Klein, P., Lis, J., Locutura, J., Marsina, K., Mazreku, A., O'Connor, P.J., Olsson, S.Å., Ottesen, R.-.T., Petersell, V., Plant, J.A., Reeder, S., Salpeteur, I., Sandström, H., Siewers, U., Steenfelt, A., Tarvainen, T., 2005. Geochemical Atlas of Europe. Part 1: Background Information, Methodology and Maps. Geological Survey of Finland, Espoo.

Schulze, T., Ulrich, M., Maier, D., Maier, M., Terytze, K., Braunbeck, T., Hollert, H., 2015. Evaluation of the hazard potentials of river suspended particulate matter and floodplain soils in the Rhine basin using chemical analysis and in vitro bioassays. Environ. Sci. Pollut. Res. 22, 14606–14620. https://doi.org/10.1007/s11356-014-3707-9.

Schumacher, M., Christl, I., Vogt, R.D., Barmettler, K., Jacobsen, C., Kretzschmar, R., 2006. Chemical composition of aquatic dissolved organic matter in five boreal forest catchments sampled in spring and fall seasons. Biogeochemistry 80, 263–275. https://doi.org/10.1007/s10533-006-9022-x.

Selomulya, C., Bushell, G., Amal, R., Waite, T.D., 2003. Understanding the role of restructuring in flocculation: the application of a population balance model. Chem. Eng. Sci. 58, 327–338. https://doi.org/10.1016/S0009-2509(02)00523-7.

Slomberg, D.L., Ollivier, P., Radakovitch, O., Baran, N., Sani-Kast, N., Miche, H., Borschneck, D., Grauby, O., Bruchet, A., Scheringer, M., Labille, J., 2016. Characterisation of suspended particulate matter in the Rhone River: insights into analogue selection. Environ. Chem. 13, 804. https://doi.org/10.1071/EN15065.

Spencer, K.L., Wheatland, J.A.T., Bushby, A.J., Carr, S.J., Droppo, I.G., Manning, A.J., 2021. A structure–function based approach to floc hierarchy and evidence for the non-fractal nature of natural sediment flocs. Sci. Rep. 11, 14012. https://doi.org/10.1038/s41598-021-93302-9.

Stone, V., Nowack, B., Baun, A., van den Brink, N., von der Kammer, F., Dusinska, M., Handy, R., Hankin, S., Hassellöv, M., Joner, E., Fernandes, T.F., 2010. Nanomaterials for environmental studies: classification, reference material issues, and strategies for

physico-chemical characterisation. Sci. Total Environ. 408, 1745–1754. https://doi.org/10.1016/j.scitotenv.2009.10.035.
Surette, M.C., Nason, J.A., 2019. Nanoparticle aggregation in a freshwater river: the role of engineered surface coatings. Environ. Sci. Nano 6, 540–553. https://doi.org/10.1039/C8EN01021H.
Svendsen, C., Walker, L.A., Matzke, M., Lahive, E., Harrison, S., Crossley, A., Park, B., Lofts, S., Lynch, I., Vázquez-Campos, S., Kaegi, R., Gogos, A., Asbach, C., Cornelis, G., von der Kammer, F., van den Brink, N.W., Mays, C., Spurgeon, D.J., 2020. Key principles and operational practices for improved nanotechnology environmental exposure assessment. Nat. Nanotechnol. 15, 731–742. https://doi.org/10.1038/s41565-020-0742-1.
Tan, Y., Kilduff, J.E., 2007. Factors affecting selectivity during dissolved organic matter removal by anion-exchange resins. Water Res. 41, 4211–4221. https://doi.org/10.1016/j.watres.2007.05.050.
Tran, D., Kuprenas, R., Strom, K., 2018. How do changes in suspended sediment concentration alone influence the size of mud flocs under steady turbulent shearing? Cont. Shelf Res. 158, 1–14. https://doi.org/10.1016/j.csr.2018.02.008.
Veerapaneni, S., Wiesner, M.R., 1996. Hydrodynamics of fractal aggregates with radially varying permeability. J. Colloid Interface Sci. 177, 45–57. https://doi.org/10.1006/jcis.1996.0005.
Velzeboer, I., Quik, J.T.K., van de Meent, D., Koelmans, A.A., 2014. Rapid settling of nanoparticles due to heteroaggregation with suspended sediment. Environ. Toxicol. Chem. 33, 1766–1773. https://doi.org/10.1002/etc.2611.
Vlieghe, M., Coufort-Saudejaud, C., Frances, C., Liné, A., 2014. In situ characterization of floc morphology by image analysis in a turbulent Taylor-Couette reactor. AIChE J. 60, 2389–2403. https://doi.org/10.1002/aic.14431.
Walch, H., von der Kammer, F., Hofmann, T., 2022. Freshwater suspended particulate matter—key components and processes in floc formation and dynamics. Water Res. 220, 118655 https://doi.org/10.1016/j.watres.2022.118655.
Wang, Hao, Zhao, X., Han, X., Tang, Z., Liu, S., Guo, W., Deng, C., Guo, Q., Wang, Huanhua, Wu, F., Meng, X., Giesy, J.P., 2017. Effects of monovalent and divalent metal cations on the aggregation and suspension of Fe3O4 magnetic nanoparticles in aqueous solution. Sci. Total Environ. 586, 817–826. https://doi.org/10.1016/j.scitotenv.2017.02.060.
Wang, W., Howe, J.Y., Gu, B., 2008. Structure and morphology evolution of hematite (α-Fe 2 O 3) nanoparticles in forced hydrolysis of ferric chloride. J. Phys. Chem. C 112, 9203–9208. https://doi.org/10.1021/jp800683j.
Wang, Z., Jin, Y., Shen, C., Li, T., Huang, Y., Li, B., 2016. Spontaneous detachment of colloids from primary energy minima by Brownian diffusion. PLoS One 11, e0147368. https://doi.org/10.1371/journal.pone.0147368.
Westerhoff, P., Nowack, B., 2013. Searching for global descriptors of engineered nanomaterial fate and transport in the environment. Acc. Chem. Res. 46, 844–853. https://doi.org/10.1021/ar300030n.
Wheatland, J.A.T., Bushby, A.J., Spencer, K.L., 2017. Quantifying the structure and composition of flocculated suspended particulate matter using focused ion beam nanotomography. Environ. Sci. Technol. 51, 8917–8925. https://doi.org/10.1021/acs.est.7b00770.
Woodward, J.C., Walling, D.E., 2007. Composite suspended sediment particles in river systems: their incidence, dynamics and physical characteristics. Hydrol. Process. 21, 3601–3614. https://doi.org/10.1002/hyp.6586.
Yu, S., Li, Q., Shan, W., Hao, Z., Li, P., Liu, J., 2021. Heteroaggregation of different surface-modified polystyrene nanoparticles with model natural colloids. Sci. Total Environ. 784, 147190 https://doi.org/10.1016/j.scitotenv.2021.147190.
Yu, W., Gregory, J., Campos, L., Li, G., 2011. The role of mixing conditions on floc growth, breakage and re-growth. Chem. Eng. J. 171, 425–430. https://doi.org/10.1016/j.cej.2011.03.098.
Zhou, D., Abdel-Fattah, A.I., Keller, A.A., 2012. Clay particles destabilize engineered nanoparticles in aqueous environments. Environ. Sci. Technol. 46, 7520–7526. https://doi.org/10.1021/es3004427.
Zimmermann-Timm, H., 2002. Characteristics, dynamics and importance of aggregates in rivers - an invited review. Int. Rev. Hydrobiol. 87, 197–240. https://doi.org/10.1002/1522-2632(200205)87:2/3<197::AID-IROH197>3.0.CO;2-7.